



CHORUS

This is the accepted manuscript made available via CHORUS. The article has been published as:

Measurement-Based Entanglement of Noninteracting Bosonic Atoms

Brian J. Lester, Yiheng Lin, Mark O. Brown, Adam M. Kaufman, Randall J. Ball, Emanuel Knill, Ana M. Rey, and Cindy A. Regal

Phys. Rev. Lett. **120**, 193602 — Published 10 May 2018

DOI: [10.1103/PhysRevLett.120.193602](https://doi.org/10.1103/PhysRevLett.120.193602)

Measurement-based entanglement of non-interacting bosonic atoms

Brian J. Lester,^{1,*} Yiheng Lin,¹ Mark O. Brown,¹ Adam M. Kaufman,¹
Randall J. Ball,¹ Emanuel Knill,^{2,3} Ana M. Rey,^{1,3} and Cindy A. Regal^{1,†}

¹*JILA, National Institute of Standards and Technology and University of Colorado,
and Department of Physics, University of Colorado, Boulder, Colorado 80309, USA*

²*National Institute of Standards and Technology, 325 Broadway, Boulder, Colorado 80305, USA*

³*Center for Theory of Quantum Matter, University of Colorado, Boulder, Colorado 80309, USA*

(Dated: April 9, 2018)

We demonstrate the ability to extract a spin-entangled state of two neutral atoms via postselection based on a measurement of their spatial configuration. Typically entangled states of neutral atoms are engineered via atom-atom interactions. In contrast, in our work we use Hong-Ou-Mandel interference to postselect a spin-singlet state after overlapping two atoms in distinct spin states on an effective beamsplitter. We verify the presence of entanglement and determine a bound on the postselected fidelity of a spin-singlet state of (0.62 ± 0.03) . The experiment has direct analogy to creating polarization entanglement with single photons, and hence demonstrates the potential to use protocols developed for photons to create complex quantum states with non-interacting atoms.

Neutral atoms have increasingly become a platform for understanding and characterizing entanglement in many-body systems and have the potential to become a resource for quantum information processing [1, 2]. The advantage of neutral atoms in quantum processing is that they can be well-isolated from the environment and transported spatially in close proximity with little unwanted interaction [2, 3]. However, the naturally small interactions that enable these traits have made creating entanglement between neutral atoms more challenging. To deterministically entangle the spin of individual neutral atoms, experimenters have used long-range interactions between Rydberg states [4–6] and the exchange interaction of atoms in their electronic ground state [7–11]. It is also possible to use photons that have interacted with individual neutral atoms or ions to entangle two atomic spins [12–16]. Many of the experiments harnessing photons to create atomic entanglement draw on the power of measurement to enable postselection or heralding, which is an increasingly common technique in atomic physics [12, 13, 17–20].

However, controlled photon-atom interactions are not required to create entanglement via measurement. Individual bosonic neutral atoms can themselves be interfered and detected, as in recent experiments that realize atom equivalents of the Hong-Ou-Mandel (HOM) effect [21, 22]. When neutral atoms are non-interacting, they can be used in place of photons in probabilistic entanglement schemes [23–27]. The additional advantage of choosing atoms is that many well-developed tools — addressability, single atom sources, high-efficiency single particle detection, long-lived memory — can be incorporated, which are not always accessible with photons. In this Letter, we show that it is possible to entangle two non-interacting ⁸⁷Rb atoms by postselecting on the spatial location of the atoms after their interference on a beamsplitter.

We implement an effective atomic beamsplitter by de-

localizing atoms between two sides of a double-well potential via a resonant tunnel-coupling [21] (Fig. 1). If the atoms are in the same spin state — meaning symmetric in both spin and space — and completely indistinguishable, one observes the HOM effect with atoms, where both atoms coalesce into the same well [1, 21, 22, 28]. If the atoms are initialized in orthogonal spin states, they are in a superposition of the symmetric and antisymmetric spin states and, correspondingly, the symmetric and antisymmetric spatial states to preserve the total symmetry of the bosonic wavefunction. Each of these evolve differently when combined on a 50:50 beamsplitter: The symmetric portion coalesces into the same well. The antisymmetric portion remains unchanged by the beamsplitter and therefore the atoms are kept in separate wells. Thus, by selecting cases where atoms remain in separate wells after the beamsplitter, the spins will be in the maximally entangled (antisymmetric) singlet state $|S_0\rangle = \frac{1}{\sqrt{2}}(|\downarrow, \uparrow\rangle - |\uparrow, \downarrow\rangle)$, where a ket with two arrows represents the joint spin state of the atoms in well 1 and well 2, respectively. We characterize the spin state after the effective beamsplitter by performing differential spin manipulations and spin-sensitive detection.

Our work is closely related to common experimental methods and proposals for optical photons. In this context, it is known that interference of identical photons and strong measurement, along with phase shifting, is in principle sufficient to generate entanglement and enact quantum gates; this is the basis for linear optical quantum computing (LOQC) [25, 29–32]. The direct optical analog to our entangling mechanism is a seminal experiment in which polarization-entangled photon states are generated by interfering two photons of orthogonal polarization on a 50:50 beamsplitter and postselecting on coincident detection in the two output modes [24]. Figure 1(c) shows the prototypical example of this experiment with linear optics, where the state is subsequently characterized using polarization-selective detec-

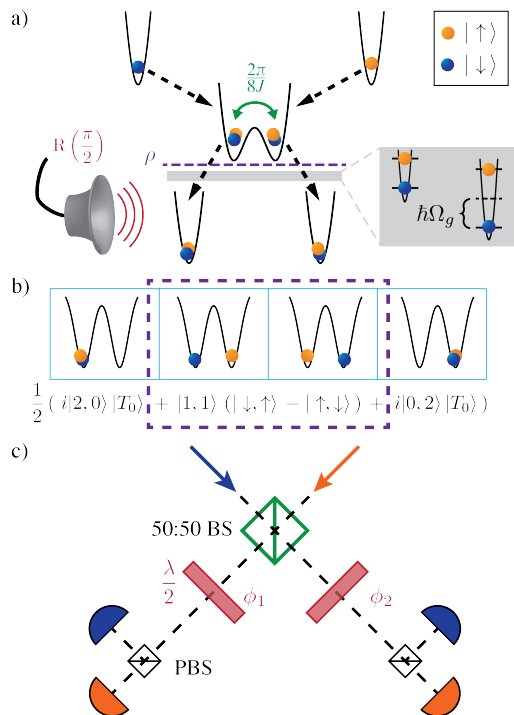


FIG. 1. Extracting entanglement through interference and postselection. a) Two bosonic atoms are prepared in orthogonal spin states and delocalized in the double-well potential to interfere the atoms via a tunnel coupling, which generates a state of interest ρ (purple dashed line). A differential spin-dependent energy shift between the wells, achieved when the wells have different depths (gray box), and a global microwave $\pi/2$ spin-rotation are used to characterize entanglement in ρ [35]. b) The four possible measurement outcomes (blue boxes). Atoms found in separate traps, i.e., in the $|1, 1\rangle$ spatial state, are in the maximally entangled singlet spin state $|S_0\rangle = \frac{1}{\sqrt{2}}(|\downarrow, \uparrow\rangle - |\uparrow, \downarrow\rangle)$ (purple dashed box). Atoms in the same well are in the symmetric (triplet) spin state $|T_0\rangle = \frac{1}{\sqrt{2}}(|\downarrow, \uparrow\rangle + |\uparrow, \downarrow\rangle)$. c) Photon analogy. Single photons with orthogonal polarization are overlapped on a 50:50 beamsplitter. When a photon is detected in each output mode, the polarization of the two photons is maximally entangled. The entanglement is characterized with independent polarization-rotations and polarization-sensitive detection [24].

tors and arbitrary polarization rotations. By comparing the coincidence counts for particular sets of path rotation angles ϕ_1 and ϕ_2 , Ref. [24] demonstrated that the correlations between the two photon polarizations violate Bell's inequalities. Here, our goal is to demonstrate that an analogous measurement-based protocol for neutral atoms generates entangled states that could be used as a resource in quantum information processing or in construction of non-trivial many-body states. Therefore, we verify spin entanglement of the two atoms by demonstrating that the singlet state fidelity \mathcal{F}_{S_0} exceeds $1/2$.

The experiment begins by isolating two single ^{87}Rb

atoms using collisional blockade in two optical tweezers separated by $d = 2.09 \mu\text{m}$ [33]. The presence (or absence) of an atom in each well of the double-well potential is recorded in an initial population image with photons collected during a period of sub-doppler cooling. This is followed by optical pumping and three-dimensional Raman sideband cooling to initialize both atoms in the $|\uparrow\rangle \equiv |F = 2, m_F = 2\rangle$ hyperfine spin state of the $5S_{1/2}$ electronic orbital and in the three-dimensional motional-ground-state in $(90 \pm 10)\%$ of trials [34]. We then initialize the atom in well 1 in the $|\downarrow\rangle \equiv |F = 1, m_F = 1\rangle$ state while keeping the atom in well 2 in $|\uparrow\rangle$. To achieve this, we take advantage of an added spin-dependence of the trapping potential (due to the vector light shift from a small component of circular polarization in the trap light) that results in a differential energy shift $\hbar\Omega_s$ of the spin transitions when the wells have different depths. For our chosen trapping depths, the $|\uparrow\rangle \leftrightarrow |\downarrow\rangle$ transition for the two atoms are spectrally resolved by $\Omega_s/2\pi = 153$ kHz, and we selectively rotate the spin of the atom in well 1 with a global microwave drive [35].

After state preparation, the separation of the optical tweezers is adiabatically changed to bring the gaussian beam centers to $d = 900$ nm, and the trap depth is reduced to $V_0/\hbar = (14.9 \pm 0.4)$ kHz per tweezer. This realizes a tunnel-coupling between well 1 and well 2 of the double-well potential with $2\hbar J$ giving the energy difference between the ground-band spatially symmetric and antisymmetric single-particle eigenstates of the double well [9, 21]. An atom initially localized in one well will be transferred to the other well with a probability that oscillates as $P_{\text{tun}}(t) = \frac{1}{2}(1 - \cos(2J(t - t_0)))$. Here t_0 is an offset that stems from the tunneling initialization. In the trap used for tunneling, the on-site interaction energy U is small enough, with $\frac{J}{U} > 3$, that the inter-particle interactions do not significantly alter tunneling dynamics [7, 21, 35, 36]. After a variable period of tunneling in the double-well potential, the trap depth is diabatically increased to at least $V_0/\hbar = 180$ kHz to freeze tunneling dynamics. It is at this point that the state ρ [purple in Fig. 1(a)] has been created; additional operations are performed to verify spin entanglement in the postselected state.

Figure 2 shows the tunneling dynamics of atoms in the double well potential to demonstrate the action of our effective atomic beamsplitter. Note that in all experiments presented in this manuscript, a global $\pi/2$ spin-rotation $\exp(-i\frac{\pi}{2}\hat{S}_x)$, where $\hat{S}_x = \frac{1}{2}(\hat{\sigma}_x^1 + \hat{\sigma}_x^2)$, is applied after the beamsplitter. This is the analog of setting the two waveplate angles in the photon experiment [Fig. 1(c)] to $\phi_1 = \phi_2 = \pi/4$. The spin rotation does not affect the population measurements, and hence is traced out in Fig. 2. It will be crucial, however, for inferring correlations from the projective spin measurements presented in Fig. 3.

Figure 2(a) shows the probability P_{10} for a trial to end in the $|1, 0\rangle$ state, where a ket $|i, j\rangle$ identifies the state with i atoms in well 1 and j atoms in well 2. The blue (orange) curve is for the subset of trials in which the initial population image records a single atom in well 1 (well 2). At $t_B = \frac{2\pi}{8J} - t_0 \simeq 0.9$ ms, the single-particle populations cross at $P_{10} = 0.5$ and the beamsplitter operation is realized. The tunneling oscillations in Fig. 2(a), which extend to times $t \gg t_B$, are indicative of the spatial coherence of the atom.

Figure 2(b) shows the corresponding probability P_{11} for a trial to end in the $|1, 1\rangle$ state for the subset of trials in which the initial population image records a single atom each in well 1 and well 2. In the ideal situation $P_{11} = \frac{1}{2} + \frac{1}{4} [1 + \cos(4J(t - t_0))]$. In our measurements we do observe that the resulting probability for the atoms to end the tunneling sequence in separate wells oscillates at $2\pi/(4J)$, but never goes below $P_{11} = 0.5$ (indicated by the purple dashed line), as expected for distinguishable bosons. The cyan dot-dashed line represents the maximum expected P_{11} based on the population dynamics measured for single-particle tunneling. Note that, for this figure only, the quantity P_{11} is corrected for single particle loss; this is because imaging can not distinguish a doubly occupied well from atom loss due to the collisional blockade [21, 35, 37].

We now focus on the measurement-based entanglement analysis that relies on postselecting the spatial state after the beam splitter action. The results are filtered to select only trials in which a single atom is recorded in each well in the initial population image and the $|1, 1\rangle$ spatial state is measured in the final imaging sequence. Filtering the trials on this condition not only removes trials where the final population is $|0, 2\rangle$ or $|2, 0\rangle$, but also removes instances where an atom is lost or the state detection protocol has an error. For example, detection errors could come from imperfect global spin-rotations or spurious large background counts. A detailed table of the possible image outcomes for a single experimental trial, as well as their interpretation in the context of this experiment, is presented in the supplementary material [35]. The postselection required for this experiment is enabled by a spin-sensitive imaging sequence that allows us to extract both spatial and spin information from each experiment trial. Two images are taken, each of which selectively measures the population in the $|\uparrow\rangle$ spin state. In between the two images, a global π spin-rotation is applied to exchange the $|\uparrow\rangle$ and $|\downarrow\rangle$ populations [35, 38, 39].

In a first experiment, we reanalyze the data used for Fig. 2(b) to study correlations in the joint spin state ρ (after postselection), as a function of the tunneling time. Specifically, we evaluate the parity of the measured spin state $\Pi = \sum_j P_j (-1)^j$, where P_j is the probability to measure j atoms in $|\uparrow\rangle$, after the global $\pi/2$ spin-rotation described above. This reanalysis gives the parity shown in Fig. 3(a), which oscillates at a frequency $4J$ with the

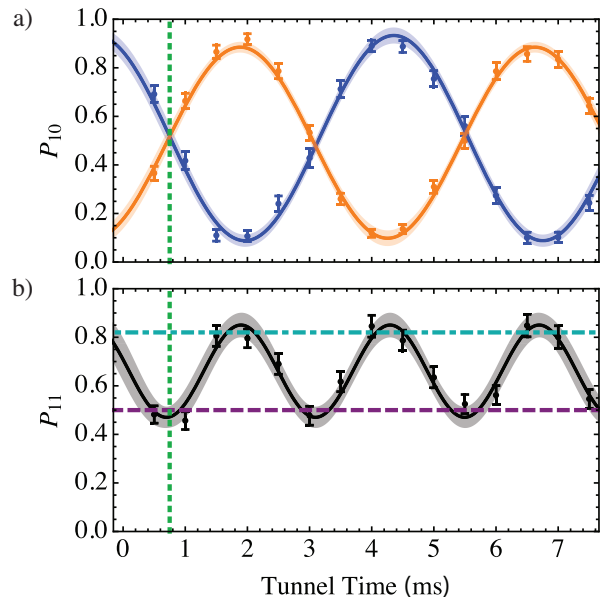


FIG. 2. a) Measured P_{10} as a function of tunneling time for a single atom initialized in $|1, 0\rangle |\downarrow\rangle$ (blue) or $|0, 1\rangle |\uparrow\rangle$ (orange). The green dotted line marks the first time the 50:50 beamsplitter is realized at time t_B . b) Measured P_{11} after initializing the state $|1, 1\rangle |\downarrow, \uparrow\rangle$. Also shown are the distinguishable atom limit (purple dashed line) and the maximum probability for the atoms to be in separate wells (dot-dashed cyan line) calculated from the single-atom tunneling contrast in (a). All data points are plotted with error bars indicating the standard error of measurement. The fits shown are performed using a standard least-squares minimization with data points weighted by their statistical error, and the shaded regions indicate the 95% confidence interval for the mean values predicted by the fits.

minima in parity coinciding with the minima in P_{11} from Fig. 2(b) (where a 50:50 beamsplitter operation is realized). With the knowledge that each spin is prepared in either $|\uparrow\rangle$ or $|\downarrow\rangle$ and that the tunneling dynamics conserve spin, we know a spin parity $\Pi \neq 0$ is evidence of correlations in the joint spin state ρ . In particular, $\Pi < 0$ indicates a non-zero projection onto $|S_0\rangle$, which is an eigenstate of the global rotation and has $\Pi = -1$ [35].

Next, for a fixed tunneling time t_B that realizes a 50:50 beamsplitter, we vary the length of time that the atoms are held in an effective magnetic field gradient between the two wells. This allows us to study the spin coherences present after the effective atomic beamsplitter. The effective gradient is provided by a spin-state-dependent relative energy shift $\hbar\Omega_g$, which is introduced with the same technique as the spin-addressing shift $\hbar\Omega_s$, but is significantly smaller with $\Omega_g/2\pi \leq 0.25$ kHz [35]. The spin-dependent energy shift results in the differential phase accumulation $\Omega_g t$ of the $|\uparrow, \downarrow\rangle$ state with respect to the $|\downarrow, \uparrow\rangle$ state [Fig. 1(a)]. This phase accumulation ideally leads to the spin state evolution $|\Psi(t)\rangle =$

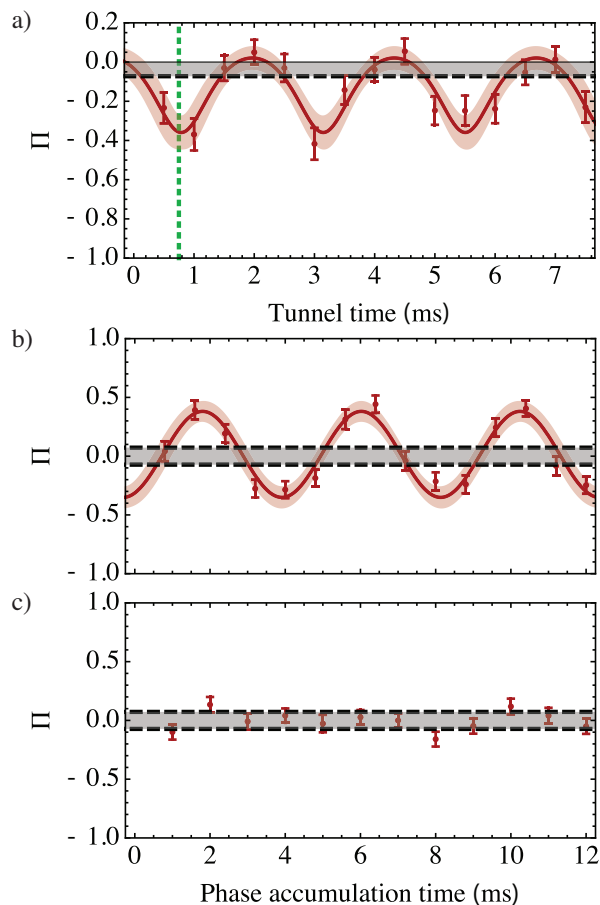


FIG. 3. Measurements of the spin parity postselected on the $|1, 1\rangle$ state after performing global microwave spin-rotations. a) Parity as a function of tunneling evolution time. The minima coincide with tunneling times t_B in Fig. 2 (green dotted lines). The functional form of the oscillations is expected due to postselection, as discussed in [35]. b) For a fixed tunneling evolution time of $t_B \simeq 0.9$ ms, a differential phase $\Omega_g t$ is accumulated between the $|\downarrow, \uparrow\rangle$ and $|\uparrow, \downarrow\rangle$ spin states before performing the global spin-rotation. For this fit, we calculate a reduced chi-squared of 1.48 with 11 degrees of freedom [35]. c) The same experiment as (b), but for a fixed tunneling time of $t \ll t_B$ for which the spins remain in a separable state. In all plots, the grey bars are a visual representation of the maximum amplitude of parity oscillations $A = \pm 2(\rho_{\uparrow\downarrow, \uparrow\downarrow} \rho_{\downarrow\uparrow, \downarrow\uparrow})^{1/2}$ that are possible for a separable density matrix, under the assumption that there are no coherences between $|\uparrow, \uparrow\rangle$ and $|\downarrow, \downarrow\rangle$. See Fig. 2 caption for explanation of error bars.

$\frac{1}{\sqrt{2}} (|\downarrow, \uparrow\rangle - e^{i\Omega_g t} |\uparrow, \downarrow\rangle)$, periodically rotating the singlet state to a triplet state $|T_0\rangle = \frac{1}{\sqrt{2}} (|\downarrow, \uparrow\rangle + |\uparrow, \downarrow\rangle)$ after a time $t = \pi/\Omega_g$. Importantly, after the global $\pi/2$ spin-rotation the $|T_0\rangle$ state has $+1$ parity, which results in the oscillation of the parity as a function of the accumulated differential phase $\Omega_g t$, as seen in Fig. 3(b). We fit the oscillation of the measured parity as $\Pi(t) = C_{\Pi} \cos(\Omega_g t + \theta_0) + p_0$, which gives $C_{\Pi} = -(0.36 \pm 0.03)$,

$\Omega_g/2\pi = (237 \pm 4)$ Hz, consistent with the expectation for Ω_g [35]. These parity oscillations will have $C_{\Pi} = -1$ for a perfect singlet state. The offsets in phase and parity are $\theta_0 = (0.46 \pm 0.19)$ and $p_0 = (0.015 \pm 0.025)$, respectively. We perform a non-parametric bootstrap analysis to check the consistency of the analysis [35]. For comparison, we perform the same set of rotations when the tunneling time is short compared to t_B , such that the spin state is primarily $|\downarrow, \uparrow\rangle$ and observe the reduced parity signal shown in Fig. 3(c).

After perfect state preparation and an ideal beamsplitter operation, the spin state postselected on the atom location $|1, 1\rangle$ will be the maximally entangled spin singlet state $|S_0\rangle$. The singlet state fidelity is a standard entanglement witness; a fidelity \mathcal{F}_{S_0} exceeding $1/2$ is sufficient to both verify entanglement and, given many copies of the same state, to distill arbitrarily good singlet states [40, 41]. Here, the fidelity is given by $\mathcal{F}_{S_0} = \langle S_0 | \rho | S_0 \rangle$, where ρ is the 4×4 density matrix of the postselected joint spin state (after the beamsplitter, but before the spin manipulations), which becomes

$$\mathcal{F}_{S_0} = \frac{1}{2} (\rho_{\uparrow\downarrow, \uparrow\downarrow} + \rho_{\downarrow\uparrow, \downarrow\uparrow}) - \text{Re}(\rho_{\uparrow\downarrow, \downarrow\uparrow}), \quad (1)$$

with $\rho_{i,j}$ indicating the density matrix elements for the possible spin configurations i and j .

These density matrix elements can be bounded by combining the measurements described above with external characterizations of our state preparation and single-spin coherence [35]. Specifically, a lower bound on the first two terms in Eqn. 1 is given by $\rho_{\uparrow\downarrow, \uparrow\downarrow} + \rho_{\downarrow\uparrow, \downarrow\uparrow} \geq (0.870 \pm 0.018)$, where the spin populations are determined by a separate measurement of the spin population after the initial state preparation. This represents a lower bound because the HOM effect results in atoms with aligned spins contributing relatively less due to postselection on $|1, 1\rangle$. The parity oscillation contrast measured in Fig. 3(b) is ideally a direct measurement of the third term in Eqn. 1, i.e., $C_{\Pi} = 2 \text{Re}(\rho_{\uparrow\downarrow, \downarrow\uparrow})$. This equality remains valid by assuming, as justified in [35], that no coherences exist between the $|\uparrow, \uparrow\rangle$ and $|\downarrow, \downarrow\rangle$ states (before the two spin manipulations). With these measurements, we calculate a postselected singlet state fidelity of $\mathcal{F}_{S_0} \geq (0.62 \pm 0.03)$.

We note that the finite contrast of the parity oscillations, while large enough to verify the presence of entanglement, indicates imperfections in the spin preparation and tunneling initialization [21]. The measured parity contrast is consistent with expectations from separate measurements of the atomic HOM interference contrast, and can be improved with higher-fidelity state preparation and tunneling procedures [35].

Through the interference of neutral atoms, we have demonstrated that postselection on the spatial configuration of atoms can be used to isolate spin-entangled states. Measurement-based schemes can be extended to

entanglement of larger and more complex systems by determining the success of the entire operation based on the final population distribution [26, 27, 32]. Alternatively, the presence of entanglement can be heralded through measurement of a subsystem, which makes the desired state available for subsequent steps in a larger protocol [42]. The simplest way to envision this possibility is to introduce a strong on-site interaction, such as through photoassociation, at the end of the protocol to expel spatial states with two atoms on a well, while leaving states with one atom per well unaffected [43]. It is also possible to herald the presence of an entangled state without adding interactions by introducing ancilla atoms and wells in analogy to demonstrations with photons [44].

We thank Michael Foss-Feig, Leonid Isaev, and Tobias Thiele. We acknowledge funding from NSF grant number PHYS 1734006, ONR grant number N00014-17-1-2245, AFOSR-MURI grant number FA9550-16-1-0323, a Cottrell Scholar award, and the Packard Foundation. AMR acknowledges funding from AFOSR FA9550-13-1-0086, AFOSR-MURI Advanced Quantum Materials, NIST and DARPA W911NF-16-1-0576 through ARO. MOB acknowledges support from an NDSEG fellowship.

* Current address: Department of Applied Physics, Yale University, New Haven, Connecticut 06520, USA; E-mail: blester@jila.colorado.edu

† E-mail: regal@colorado.edu

- [1] R. Islam, R. Ma, P. M. Preiss, M. E. Tai, A. Lukin, M. Rispoli, and M. Greiner, “Measuring entanglement entropy in a quantum many-body system,” *Nature (London)* **528**, 77 (2015).
- [2] D. S. Weiss and M. Saffman, “Quantum computing with neutral atoms,” *Phys. Today* **70**, 44 (2017).
- [3] C. Weitenberg, S. Kuhr, K. Mølmer, and J. F. Sherson, “Quantum computation architecture using optical tweezers,” *Phys. Rev. A* **84**, 032322 (2011).
- [4] T. Wilk, A. Gaëtan, C. Evellin, J. Wolters, Y. Miroshnychenko, P. Grangier, and A. Browaeys, “Entanglement of Two Individual Neutral Atoms Using Rydberg Blockade,” *Phys. Rev. Lett.* **104**, 010502 (2010).
- [5] L. Isenhower, E. Urban, X. L. Zhang, A. T. Gill, T. Henage, T. A. Johnson, T. G. Walker, and M. Saffman, “Demonstration of a Neutral Atom Controlled-NOT Quantum Gate,” *Phys. Rev. Lett.* **104**, 010503 (2010).
- [6] M. Saffman, T. Walker, and K. Mølmer, “Quantum information with Rydberg atoms,” *Rev. Mod. Phys.* **82**, 2313 (2010).
- [7] A. M. Kaufman, B. J. Lester, M. Foss-Feig, M. L. Wall, A. M. Rey, and C. A. Regal, “Entangling two transportable neutral atoms via local spin exchange,” *Nature (London)* **527**, 208 (2015).
- [8] T. Fukuhara, S. Hild, J. Zeiher, P. Schauß, I. Bloch, M. Endres, and C. Gross, “Spatially Resolved Detection of a Spin-Entanglement Wave in a Bose-Hubbard Chain,” *Phys. Rev. Lett.* **115**, 035302 (2015).
- [9] S. Murmann, A. Bergschneider, V. M. Klinkhamer, G. Zürn, T. Lompe, and S. Jochim, “Two Fermions in a Double Well: Exploring a Fundamental Building Block of the Hubbard Model,” *Phys. Rev. Lett.* **114**, 080402 (2015).
- [10] M. Anderlini, P. J. Lee, B. L. Brown, J. Sebby-Strabley, W. D. Phillips, and J. V. Porto, “Controlled Exchange Interaction Between Pairs of Neutral Atoms in an Optical Lattice,” *Nature (London)* **448**, 452 (2007).
- [11] S. Trotzky, P. Cheinet, S. Fölling, M. Feld, U. Schnorrberger, A. M. Rey, A. Polkovnikov, E. A. Demler, M. D. Lukin, and I. Bloch, “Time-resolved Observation and Control of Superexchange Interactions with Ultracold Atoms in Optical Lattices,” *Science* **319**, 295 (2008).
- [12] D. L. Moehring, P. Maunz, S. Olmschenk, K. C. Younge, D. N. Matsukevich, L. M. Duan, and C. Monroe, “Entanglement of single-atom quantum bits at a distance,” *Nature (London)* **449**, 68 (2007).
- [13] J. Hofmann, M. Krug, N. Ortegel, L. Gerard, M. Weber, W. Rosenfeld, and H. Weinfurter, “Heralded Entanglement Between Widely Separated Atoms,” *Science* **337**, 72 (2012).
- [14] S. Ritter, C. Nölleke, C. Hahn, A. Reiserer, A. Neuzner, M. Uphoff, M. Mücke, E. Figueroa, J. Bochmann, and G. Rempe, “An elementary quantum network of single atoms in optical cavities,” *Nature (London)* **484**, 195 (2012).
- [15] B. Casabone, A. Stute, K. Friebe, B. Brandstätter, K. Schüppert, R. Blatt, and T. E. Northup, “Heralded entanglement of two ions in an optical cavity,” *Phys. Rev. Lett.* **111**, 100505 (2013).
- [16] S. Welte, B. Hacker, S. Daiss, S. Ritter, and G. Rempe, “Cavity carving of atomic bell states,” *Phys. Rev. Lett.* **118**, 210503 (2017).
- [17] C. Chou, H. de Riedmatten, D. Felinto, S. Polyakov, S. van Enk, and H. Kimble, “Measurement-induced entanglement for excitation stored in remote atomic ensembles,” *Nature (London)* **438**, 828 (2005).
- [18] M. Lettner, M. Mücke, S. Riedl, C. Vo, C. Hahn, S. Baur, J. Bochmann, S. Ritter, S. Durr, and G. Rempe, “Remote entanglement between a single atom and a bose-einstein condensate,” *Phys. Rev. Lett.* **106**, 210503 (2011).
- [19] I. D. Leroux, M. H. Schleier-Smith, and V. Vuletić, “Implementation of cavity squeezing of a collective atomic spin,” *Phys. Rev. Lett.* **104**, 073602 (2010).
- [20] J. G. Bohnet, K. C. Cox, M. A. Norcia, J. M. Weiner, Z. Chen, and J. K. Thompson, “Reduced spin measurement back-action for a phase sensitivity ten times beyond the standard quantum limit,” *Nat. Photonics* **8**, 731 (2014).
- [21] A. M. Kaufman, B. J. Lester, C. M. Reynolds, M. L. Wall, M. Foss-Feig, K. R. A. Hazzard, A. M. Rey, and C. A. Regal, “Two-particle quantum interference in tunnel-coupled optical tweezers,” *Science* **345**, 306 (2014).
- [22] R. Lopes, A. Imanaliev, A. Aspect, M. Cheneau, D. Boiron, and C. I. Westbrook, “Atomic Hong-Ou-Mandel experiment,” *Nature (London)* **520**, 66 (2015).
- [23] Z. Y. Ou and L. Mandel, “Violation of bell’s inequality and classical probability in a two-photon correlation experiment,” *Phys. Rev. Lett.* **61**, 50 (1988).
- [24] Y. H. Shih and C. O. Alley, “New Type of Einstein-Podolsky-Rosen-Bohm Experiment Using Pairs of Light

- Quanta Produced by Optical Parametric Down Conversion,” *Phys. Rev. Lett.* **61**, 2921 (1988).
- [25] E. Knill, R. Laflamme, and G. J. Milburn, “A scheme for efficient quantum computation with linear optics,” *Nature (London)* **409**, 46 (2001).
- [26] P. Kok, W. J. Munro, K. Nemoto, T. C. Ralph, J. P. Dowling, and G. J. Milburn, “Linear optical quantum computing with photonic qubits,” *Rev. Mod. Phys.* **79**, 135 (2007).
- [27] J.-W. Pan, Z.-B. Chen, C.-Y. Lu, H. Weinfurter, A. Zeilinger, and M. Zukowski, “Multiphoton entanglement and interferometry,” *Rev. Mod. Phys.* **84**, 777 (2012).
- [28] P. M. Preiss, R. Ma, M. E. Tai, A. Lukin, M. Rispoli, P. Zupancic, Y. Lahini, R. Islam, and M. Greiner, “Strongly correlated quantum walks in optical lattices,” *Science* **347**, 1229 (2015).
- [29] M. A. Nielsen and I. L. Chuang, *Quantum Computation and Quantum Information* (Cambridge University Press, 2000).
- [30] S. Barz, J. F. Fitzsimons, E. Kashefi, and P. Walther, “Experimental verification of quantum computation,” *Nat. Phys.* **9**, 727 (2013).
- [31] N. Spagnolo, C. Vitelli, M. Bentivegna, D. J. Brod, A. Crespi, F. Flamini, S. Giacomini, G. Milani, R. Ramponi, P. Mataloni, R. Osellame, E. F. Galvao, and F. Sciarrino, “Experimental validation of photonic boson sampling,” *Nat. Photonics* **8**, 615 (2014).
- [32] J. Carolan, C. Harold, C. Sparrow, E. Martin-Lopez, N. J. Russell, J. W. Silverstone, P. J. Shadbolt, N. Matsuda, M. Oguma, M. Itoh, G. D. Marshall, M. G. Thompson, J. C. F. Matthews, T. Hashimoto, J. L. O’Brien, and A. Laing, “Universal linear optics,” *Science* **349**, 711 (2015).
- [33] N. Schlosser, G. Reymond, I. Protsenko, and P. Grangier, “Sub-poissonian loading of single atoms in a microscopic dipole trap,” *Nature (London)* **411**, 1024 (2001).
- [34] A. M. Kaufman, B. J. Lester, and C. A. Regal, “Cooling a Single Atom in an Optical Tweezer to Its Quantum Ground State,” *Phys. Rev. X* **2**, 041014 (2012).
- [35] See Supplementary Material at [*URL to be inserted*] for additional details on the experimental methods, data analysis techniques, and results. The Supplementary Material also includes the additional Refs. [45–49].
- [36] M. L. Wall, K. R. A. Hazzard, and A. M. Rey, “Effective many-body parameters for atoms in nonseparable Gaussian optical potentials,” *Phys. Rev. A* **92**, 013610 (2015).
- [37] N. Schlosser, G. Reymond, and P. Grangier, “Collisional Blockade in Microscopic Optical Dipole Traps,” *Phys. Rev. Lett.* **89**, 023005 (2002).
- [38] M. J. Gibbons, C. D. Hamley, C.-Y. Shih, and M. S. Chapman, “Nondestructive Fluorescent State Detection of Single Neutral Atom Qubits,” *Phys. Rev. Lett.* **106**, 133002 (2011).
- [39] A. Fuhrmanek, R. Bourgain, Y. R. P. Sortais, and A. Browaeys, “Free-Space Lossless State Detection of a Single Trapped Atom,” *Phys. Rev. Lett.* **106**, 133003 (2011).
- [40] R. Horodecki, P. Horodecki, M. Horodecki, and K. Horodecki, “Quantum entanglement,” *Rev. Mod. Phys.* **81**, 865 (2009).
- [41] C. H. Bennett, G. Brassard, S. Popescu, B. Schumacher, J. A. Smolin, and W. K. Wootters, “Purification of noisy entanglement and faithful teleportation via noisy channels,” *Phys. Rev. Lett.* **76**, 722–725 (1996).
- [42] T. B. Pittman, M. M. Donegan, M. J. Fitch, B. C. Jacobs, J. D. Franson, P. Kok, H. Lee, and J. P. Dowling, “Heralded two-photon entanglement from probabilistic quantum logic operations on multiple parametric down-conversion sources,” *IEEE Journal of Selected Topics in Quantum Electronics* **9**, 1478 (2003).
- [43] W. C. Stwalley and H. Wang, “Photoassociation of Ultracold Atoms: A New Spectroscopic Technique,” *J. Mol. Spectrosc.* **195**, 194–228 (1999).
- [44] Q. Zhang, X.-H. Bao, C.-Y. Lu, X.-Q. Zhou, T. Yang, T. Rudolph, and J.-W. Pan, “Demonstration of a scheme for the generation of “event-ready” entangled photon pairs from a single-photon source,” *Phys. Rev. A* **77**, 062316 (2008).
- [45] N. R. Hutzler, L. R. Liu, Y. Yu, and K.-K. Ni, “Eliminating light shifts for single atom trapping,” *New J. Phys.* **19**, 023007 (2017).
- [46] J. Weiner, V. S. Bagnato, S. Zilio, and P. S. Julienne, “Experiments and theory in cold and ultracold collisions,” *Rev. Mod. Phys.* **71**, 1 (1999).
- [47] T. Grunzweig, A. Hilliard, M. McGovern, and M. F. Andersen, “Near-deterministic preparation of a single atom in an optical microtrap,” *Nat. Phys.* **6**, 951 (2010).
- [48] B. J. Lester, N. Luick, A. M. Kaufman, C. M. Reynolds, and C. A. Regal, “Rapid Production of Uniformly Filled Arrays of Neutral Atoms,” *Phys. Rev. Lett.* **115**, 073003 (2015).
- [49] B. Efron and R. J. Tibshirani, *An Introduction to the Bootstrap: Monographs on Statistics and Applied Probability* (Chapman and Hall/CRC, New York and London, 1993).